

An improved BK sub-triangle product approach for scene classification

Ekta Vats*, Chee Kau Lim and Chee Seng Chan

Center of Image and Signal Processing, Faculty of Comp. Sci. & Info. Tech., University of Malaya, Kuala Lumpur, Malaysia

Abstract. Scene classification is a popular research topic in computer vision, and has received much attention in the recent past. Conventionally, scene classes are considered to be mutually exclusive. However, in real-world scenarios a scene image may belong to multiple classes, depending upon different perceptions of the masses. In this paper, we propose an improved Bandler and Kohout's sub-triangle product (BK subproduct) approach to address this issue. Instead of using the original BK subproduct solely, we introduce a combination of inference structures. The advantages are three-fold. Firstly, using the BK subproduct as an inference engine, we are able to attain the relationships between image data sets and scene classes that are not directly associated. Secondly, our approach is able to model non-mutually exclusive data, as opposed to conventional solutions. Finally, our classification result is not binary. Instead, we can classify each scene image as belonging to multiple distinct scene classes. Experimental results on public datasets demonstrate the effectiveness of the proposed method.

Keywords: BK sub-triangle product, scene classification, inference structure, fuzzy implication operator

1. Introduction

Understanding and interpreting a natural scene is a challenging task in the computer vision community because of the variability, ambiguity, illumination and scale conditions that can exist in the scene images. A scene composes of several objects is usually organized in an unpredictable layout. Oliva and Torralba [18] proposed a set of perceptual dimensions (naturalness, openness, roughness, expansion and ruggedness) to represent the dominant spatial structure of a scene and employed Support Vector Machine (SVM) classifier with Gaussian kernel to classify the scene classes; while Bosch et al. [5] proposed probabilistic Latent Semantic Analysis (pLSA) incorporated with the K-nearest neighbour classifier. Inspired by [5], a Bayesian

hierarchical model was proposed by Li and Perona [12]. Kumar et al. [15] employed graphical models to detect and localize man-made features in a scene. The concept of occurring frequency of different concepts was used by Vogel and Schiele [23, 24] as the intermediate feature for the scene classification.

Despite all the mentioned methods had achieved promising results, we observed that classification errors often occur when there is an overlap between the scene classes in the selected feature space. The reason is because all these solutions assume that the scene classes are mutually exclusive, and so their systems learn patterns from a training set and search for the images similar to it. Fig. 1 explains this scenario. In Fig. 1b it is unclear that it is an *open country* scene or a *coast* scene where different people may respond inconsistently. Therefore, we argued that the scene classes are non-mutually exclusive. This is also stated in the work conducted by Lim et al. [17].

In this paper, we propose to utilize the BK subproduct to tackle this issue, as an extension to our previous work

*Corresponding author. Ekta Vats, Center of Image and Signal Processing, Faculty of Comp. Sci. & Info. Tech., University of Malaya, 50603 Kuala Lumpur, Malaysia. Tel./Fax: 603 7967 6433; E-mail: ektavats_2608@siswa.um.edu.my.

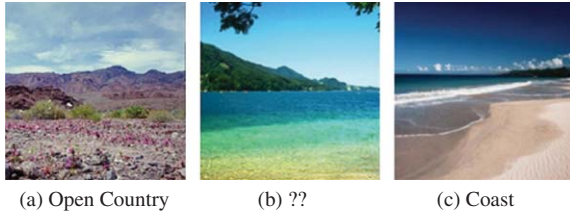


Fig. 1. Example of ambiguous scene images. What is the class for (b)? (Image best viewed in colors.)

[22]. Bandler and Kohout [1] proposed that the relations between two indirectly associated sets could be studied with the relational products. In the literature, these relational products are known as the BK relational products. A BK relational product defines the relationship between the elements within two indirectly associated sets as the overlapping of their images in a common set. In this work, we employed a series of computer vision techniques and online surveys to compute the relational products of an image and its scene classes. Our proposed classification method is closely related to some of the approximate reasoning methods which have been developed in the recent years, more specifically [3, 7]. Barrenechea et al. in [3] presented a fuzzy reasoning method in which the Choquet integral is used as an aggregation function for the rule-based classification systems. Wide benchmarks of numerical datasets were used to test the classification performance. However, their classification results are binary, allowing an element in the dataset to be belonged to a single class only. Contrary, our method deals with the multi-class, multi-label classification problem, wherein the driving force lies in the fact that the scene classes are non-mutually exclusive. Nonetheless, rule-based systems require the expert knowledge in designing the rules for the system, and the BK subproduct approach which is based on the study of the relationships between different fuzzy sets can provide a better alternative, closer to the natural solution. Bustince et al. in [7] presented a study on the implication operators. In our work, we utilized the fuzzy implication operators for scene classification.

The closest research to ours is by Lim et al. [17] where they incorporated fuzzy qualitative approach to address the problem. However, our method is much closer to a natural solution in the sense that the BK subproduct inference mechanism is a flexible and efficient method that can be employed in the real-world scenarios as it imitates how human think in the real life, i.e. modus-ponen way (if A implies B ,

A is asserted to be true, so therefore B must be true) [13]. Our main contributions are: firstly, we show that the scene images are non-mutually exclusive; and describe a BK subproduct approach for this purpose. Secondly, we present an improvised BK subproduct approach that incorporates inference structures K7 and K9 for scene classification. From the best of our knowledge, this is the first attempt that employs fuzzy BK subproduct in scene classification problem. Most of the fuzzy image processing works have been focusing on object recognition [10, 27], colour clustering [8], edge detection [4], threshold segmentation [19], human motion analysis [20], and etc.

The rest of the paper is organized as follows. Section 2 revisits the definition of BK relational products for crisp relations and an extension to the fuzzy BK subproduct. In Section 3, the application of BK subproduct in scene classification is described. Section 4 presents the empirical results using a standard dataset, and we conclude with the suggestions on the future work in Section 5.

2. BK subproduct revisit

2.1. BK subproduct for crisp relations

BK subproduct is a study of compositions of relations between sets first proposed in [1]. It can be defined in terms of crisp relations as well as fuzzy relations. To make this revisit section as self-contained as possible, we start with BK subproduct in crisp relations.

Assume that there are 3 sets, $A = \{a_i | i = 1, \dots, I\}$, $B = \{b_j | j = 1, \dots, J\}$ and $C = \{c_k | k = 1, \dots, K\}$. If R is defined as a relation between A and B such that $R \subseteq \{(a, b) | (a, b) \in A \times B\}$, we can define an image of a in B under relation R as aR :

$$aR = \{b | b \in B \text{ and } aRb\} \quad (1)$$

where aRb is an abbreviation for $(a, b) \in R$. On the other hand, if S is a relation between B and C such that $S \subseteq \{(b, c) | (b, c) \in B \times C\}$, S^C is the converse relation of S . We can define the image of an element c in set B under relation S^C as Sc :

$$Sc = \{b | b \in B \text{ and } bSc\} \quad (2)$$

where bSc is an abbreviation for $(b, c) \in S$.

With (1) and (2), we can define the indirect relations between A and C with the BK subproduct as:

$$R \triangleleft S = \{(a, c) | (a, c) \in A \times C \text{ and } aR \subseteq Sc\} \quad (3)$$

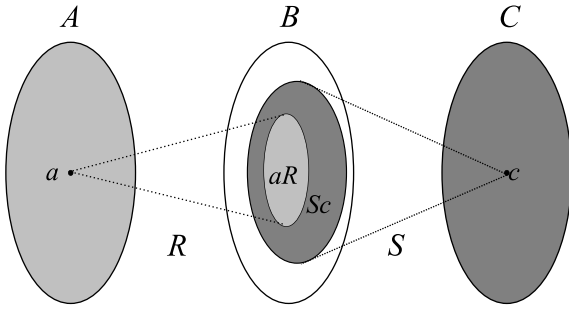


Fig. 2. Element a is in relation with c if its image under R is a subset of image Sc .

The BK subproduct gives all (a, c) couples such that the image of a under relation R in B is among the subset of c under Sc in B as illustrated in Fig. 2. For example, let A is a set of patients, B is a set of sickness signs/symptoms and C is a set of diseases. For a patient a , relation R provides the sickness signs/symptoms that diagnosed from the patient a (aR), while S shows the sickness signs/symptoms that cause a disease c , so we can conclude that the patient a may suffer from the disease c .

2.2. Fuzzy BK subproduct

Although BK subproduct is very useful, it suffers from vagueness and uncertainty issues. So, Kohout and Bandler [1] extended the crisp BK subproduct to the fuzzy BK subproduct to cope with these limitations. As one can observe in (3), $aR \subseteq Sc$ is the main element in retrieving the relationship between a and c . Thus, the subsethood measure theory is an important aspect for the fuzzy BK subproduct.

Kohout and Bandler [2] developed the fuzzy subsethood measure based on the fuzzy implication operators as shown in Table 1. For two fuzzy subsets P and Q in the universe X , where x is a general notation of elements in this universe, the possibility that P is a subset of Q is given as:

$$\pi(P \subseteq Q) = \bigwedge_{x \in X} (\mu_P(x) \rightarrow \mu_Q(x)) \quad (4)$$

where \bigwedge can be defined as the infimum operator in harsh criterion or the arithmetic mean in mean criterion; $\mu_P(x)$ and $\mu_Q(x)$ are the membership functions of x in P and Q respectively; \rightarrow represents the fuzzy implication operator.

Table 1
Example of the fuzzy implication operators and their respective definitions

Name	Symbol	Definition
S# - Standard Sharp	$r \rightarrow_{S\#} s$	$\begin{cases} 1 & \text{iff } r \neq 1 \text{ or } s = 1 \\ 0 & \text{otherwise} \end{cases}$
S - Standard Strict	$r \rightarrow_S s$	$\begin{cases} 1 & \text{iff } r \leq 1 \\ 0 & \text{otherwise} \end{cases}$
S* - Standard Star	$r \rightarrow_{S^*} s$	$\begin{cases} 1 & \text{iff } r \leq s \\ s & \text{otherwise} \end{cases}$
G43 - Gaines 43	$r \rightarrow_{G43} s$	$\min\left(1, \frac{r}{s}\right)$
G43' - Modified Gaines 43	$r \rightarrow_{KD} s$	$\min\left(1, \frac{r}{s}, \frac{1-r}{1-s}\right)$
KD - Kleene-Dienes	$r \rightarrow_{KD} s$	$\max(s, 1-r)$
R - Reichenbach	$r \rightarrow_R s$	$1-r+rs$ $= \min(1, 1-r+s)$
L - Lukasiewicz	$r \rightarrow_L s$	$\min(1, 1-r+s)$
EZ - Early Zadeh	$r \rightarrow_{EZ} s$	$(r \wedge s) \vee (1-r)$

Given (3) and (4), [1] defined the composition of relations between $a_i \in A$ and $c_k \in C$ as follows:

$$R \triangleleft S(a, c) = \bigwedge_{b \in B} (R_{ab} \rightarrow S_{bc}) \quad (5)$$

where, R_{ab} is the membership function of the relation R between a and b ; S_{bc} is the membership function of the relation S between b and c . Studies [11, 14] also found that among all the fuzzy implication operators, Reichenbach fuzzy implication operator gives the expected values in the subsethood measurement. However, in [9] De Baets and Kerre found that even if $a = a'$ has no image under relation R in set B , a' is still in relation $R \triangleleft S$ with all $c \in C$, because $\emptyset \subseteq Sc$. This limitation was studied and improved by reinforcing the non-emptiness condition:

$$R \triangleleft_K S = \{(a, c) | (a, c) \in A \times C \text{ and } \emptyset \subseteq aR \subseteq Sc\} \quad (6)$$

$$R \triangleleft_K S(a, c) = \min\left(\bigwedge_{b \in B} (R_{ab} \rightarrow S_{bc}), \bigvee_{b \in B} \tau(R_{ab}, S_{bc})\right) \quad (7)$$

where \bigvee is the supremum operator and τ is the t-norm. To apply (7) into real-world applications, operators such as \wedge , \bigvee as well as the t-norm must be defined where [25, 26] developed a list of inference structures. A study [16] found that not all of these inference structures are reliable and stated only the inference structures K7 and K9 delivered good performance. The definitions of K7 and K9 are as follows:

$$K_7 : R \triangleleft_{K7} S(a, c) = \min \left(\frac{1}{J} \sum_{b \in B} (R_{ab} \rightarrow S_{bc}), \text{OrBot}(\text{AndBot}(R_{ab}, S_{bc})) \right) \quad (8)$$

$$K_9 : R \triangleleft_{K9} S(a, c) = \min \left(\text{AndTop}(R_{ab} \rightarrow S_{bc}), \text{OrBot}(\text{AndBot}(R_{ab}, S_{bc})) \right) \quad (9)$$

where AndTop, AndBot and OrBot are the logical connectives defined as:

$$\text{AndTop}(p, q) = \min(p, q) \quad (10)$$

$$\text{AndBot}(p, q) = \max(0, p + q - 1) \quad (11)$$

$$\text{OrBot}(p, q) = \min(1, p + q) \quad (12)$$

In this paper, the inference structure instantiated from the original BK subproduct:

$$BK : R \triangleleft_{BK} S(a, c) = \frac{1}{J} \sum_{b \in B} (R_{ab} \rightarrow S_{bc}) \quad (13)$$

will be applied along with the combination of K7 and K9 to compare the results.

3. Scene classification using fuzzy BK subproduct

In this section, we describe how the fuzzy BK subproduct is employed in scene classification problem. Let us denote $A = \{a_i | i = 1, \dots, I\}$ as a set of scene images, $B = \{b_j | j = 1, \dots, J\}$ as a set of features extracted from the image frames, and $C = \{c_k | k =$

$1, \dots, K\}$ as a set of scene classes. A has no direct relation with C . However, if there exists an intermediate set B , which is in relation with both A and C , we can derive the indirect relationship between A and C using the fuzzy BK subproduct (13), along with the combination of (8) and (9), and utilize this information to classify different scene images.

First of all, for each image $a \in A$, several local patches are extracted and then represented in a 128-dimensional numerical vectors (V_1, V_2, \dots, V_{128}) using the Scale Invariant Feature Transform (SIFT) descriptors. This is to find the best features that govern the image. By doing so, each image a is represented by a set of vectors $a' \in A'$, as depicted in Fig. 3. Instead of directly using the relation $R \subseteq A \times B$, we replace R with R' where $R' \subseteq A' \times B$.

After that, k-means clustering is performed to group similar features found on each of the image a . As a result, set B is generated and labeled using an open annotation tool *LabelMe* [21], as illustrated in Fig. 4. To find the relation R' , we computed the membership function values by calculating the distribution of each feature in the image. A total of nine distinct features namely, *sand, water, sky, tree, mountain, vehicle, road, building* and *people* were identified. An example of the membership function R' for ten example images from the *coast* scene is shown in Table 2. From here, we can notice that those major features that represent *coast* scene are *water* and *sky*, while *sand, tree* and *mountain* are the minor features.

Finally, in order to find the relation S denotes the membership function between the image features and the scene classes, we employ an online survey where each human subject is given a series of image features, and asked to perform scene classification. This is in contrast to the conventional solutions [5, 12, 15, 18, 23, 24]

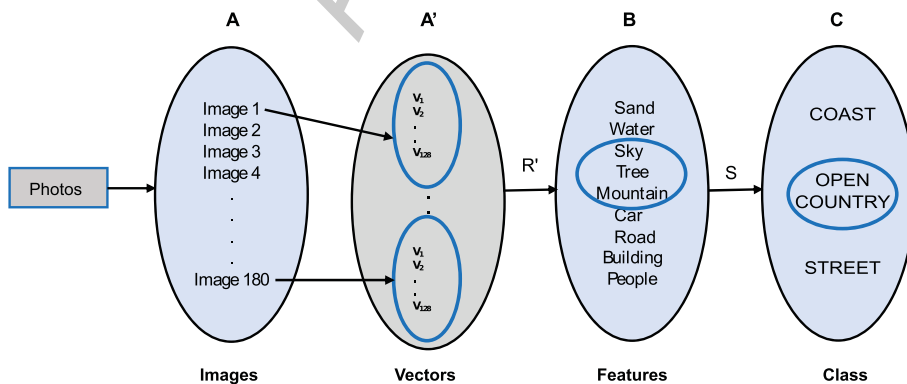


Fig. 3. An example of BK subproduct approach towards scene classification.

Fig. 4. An example of the annotated images from *coast* scene employing *Labelme* [21].Table 2
Membership functions for relation R'

Images	Sand	Water	Sky	Tree	Mountain	Vehicle	Road	Building	People
Image 1	0.00	0.45	0.415	0.00	0.003	0.102	0.00	0.000	0.03
Image 2	0.00	0.51	0.49	0.00	0.00	0.00	0.00	0.00	0.00
Image 3	0.00	0.50	0.26	0.00	0.19	0.00	0.00	0.05	0.00
Image 4	0.00	0.42	0.55	0.00	0.03	0.00	0.00	0.00	0.00
Image 5	0.00	0.56	0.254	0.046	0.14	0.00	0.00	0.00	0.00
Image 6	0.24	0.16	0.41	0.19	0.00	0.00	0.00	0.00	0.00
Image 7	0.08	0.32	0.44	0.16	0.00	0.00	0.00	0.00	0.00
Image 8	0.39	0.42	0.19	0.00	0.00	0.00	0.00	0.00	0.00
Image 9	0.00	0.58	0.24	0.00	0.18	0.00	0.00	0.00	0.00
Image 10	0.00	0.38	0.42	0.00	0.20	0.00	0.00	0.00	0.00

that learned a binary classifier with the assumption that the scene classes are mutually exclusive.

4. Experimental results

In order to test the effectiveness of our proposed framework, we employed the public dataset: Outdoor Scene Recognition (OSR) [18]. A total of three scene classes namely, *coast*, *open country* and *street* were used throughout the experiments. Figure 5 shows some example of the scene classes in gray scaled. Each scene class has 60 images, and therefore there are 180 images in total. In each scene class, 40 images are used for training and the rest are for testing. The SVM implementation is based on the LIBSVM toolbox.

4.1. Finding the relational products

As mentioned earlier, different people tend to respond inconsistently even given a same scene image. Therefore, it is plausibly possible for an image to belong to multiple classes. Herein, we conducted a survey on 200 people via social media website to gain understanding on how different people classify features into scene classes. Each subject was given a choice of nine image features (*sand*, *water*, *sky*, *tree*, *mountain*, *vehicle*, *road*, *building* and *people*). The outcome are represented in Fig. 6 where X-axis denotes the image features and Y-axis denotes the number of people in percentage. Upon on analyzing the results in Fig. 6, we observed that



(a) Example of coast scene



(b) Example of open country scene



(c) Example of street scene

Fig. 5. Examples of scene classes in the OSR Dataset [18].

the features *sky*, *tree*, *mountain* and *sand* are present in both *open country* and *coast* scenes in different magnitudes, causing them to be related to one another in some degrees. On the other hand, *street* scene is governed by *vehicle*, *road* and *building*. The relational products of S from the survey are shown in Table 3.

4.2. Scene classification using BK subproduct and comparison with K7 and K9

In this subsection, we show the results of the proposed approach that use a combination of original BK

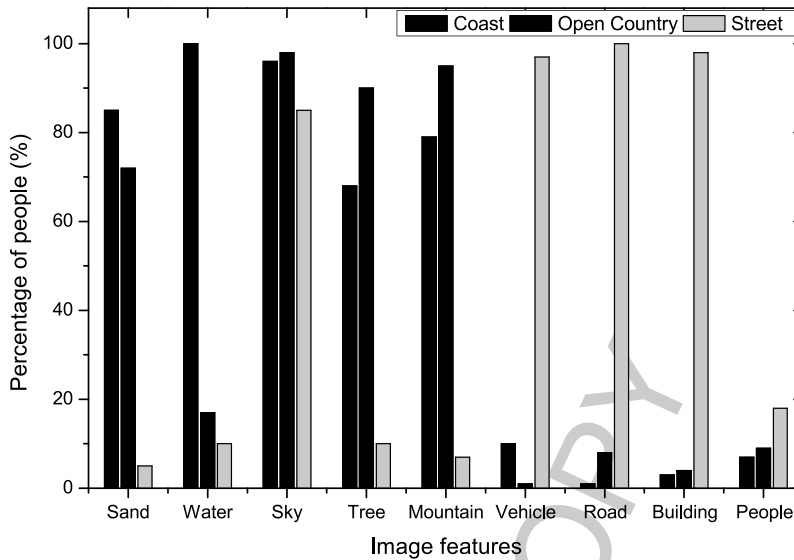


Fig. 6. Bar chart representing the results from the online survey on 200 people.

Table 3
Membership functions for relation S

Features	Coast	Open country	Street
Sand	0.55	0.35	0.00
Water	1.00	0.10	0.02
Sky	1.00	1.00	0.87
Tree	0.25	0.72	0.17
Mountain	0.45	0.60	0.02
Vehicle	0.12	0.00	0.80
Road	0.00	0.02	0.95
Building	0.05	0.05	1.00
People	0.15	0.10	0.30

subproduct with K7 and K9 inference structures, and a comparison with the conventional BK subproduct solution. We defined a dynamic threshold value to each of the scene classes and classified the number of images accepted as well as rejected, as in Tables 4–6, respectively.

From Tables 4–6, it is observed that the BK subproduct has very low discrimination power as compared to K7 and K9 respectively. The BK subproduct accepts and rejects all the *coast* images as *open country* scene

class as well as *street* scene class. For each of the *coast* images to be accepted and rejected as *open country*, this scenario is possible as proved in Fig. 7 and Table 7, respectively. Quantitatively, we showed that these two images are very much correlated as shown in Table 7, as both scene images share some common features such as *water*, *sky*, *tree* and *mountain*. Nonetheless, qualitatively, we also showed that it is very hard for a human being to distinguish the scene class of these two scene images as depicted in Fig. 7. However, the BK subproduct also accepts and rejects all the *coast* images as *street* class. From our investigation as shown in Table 8, this scenario is impossible as there are no common features that are shared by *coast* and *street*. One of the main reasons that the BK subproduct was not able to distinguish between the *coast* and *street* class is due to $\emptyset \subseteq Sc$ as identified by [16]. We also notice that *vehicle*, *road*, *building* and *people* for both *coast* and *street* scene are empty sets.

A further investigation was performed as shown in Fig. 8 and Table 8, respectively. Qualitatively from Fig. 8, it is very clear that one of the images is *coast*

Table 4
Test results for all the scenes against coast scene class

Coast (Threshold = 0.7)	Accept Original BK	Accept K7	Accept K9	Reject Original BK	Reject K7	Reject K9
Coast	20	17	20	0	3	0
Open Country	20	4	14	0	16	6
Street	20	0	5	0	20	15

Table 5
Test results for all the scenes against open country scene class

Open Country (Threshold = 0.6)	Accept Original BK	Accept K7	Accept K9	Reject Original BK	Reject K7	Reject K9
Coast	20	1	19	0	19	1
Open Country	20	4	19	0	16	1
Street	20	0	4	0	20	16

Table 6
Test results for all the scenes against street scene class

Street (Threshold = 0.5)	Accept Original BK	Accept K7	Accept K9	Reject Original BK	Reject K7	Reject K9
Coast	20	0	4	0	20	16
Open Country	20	0	1	0	20	19
Street	20	20	20	0	0	0

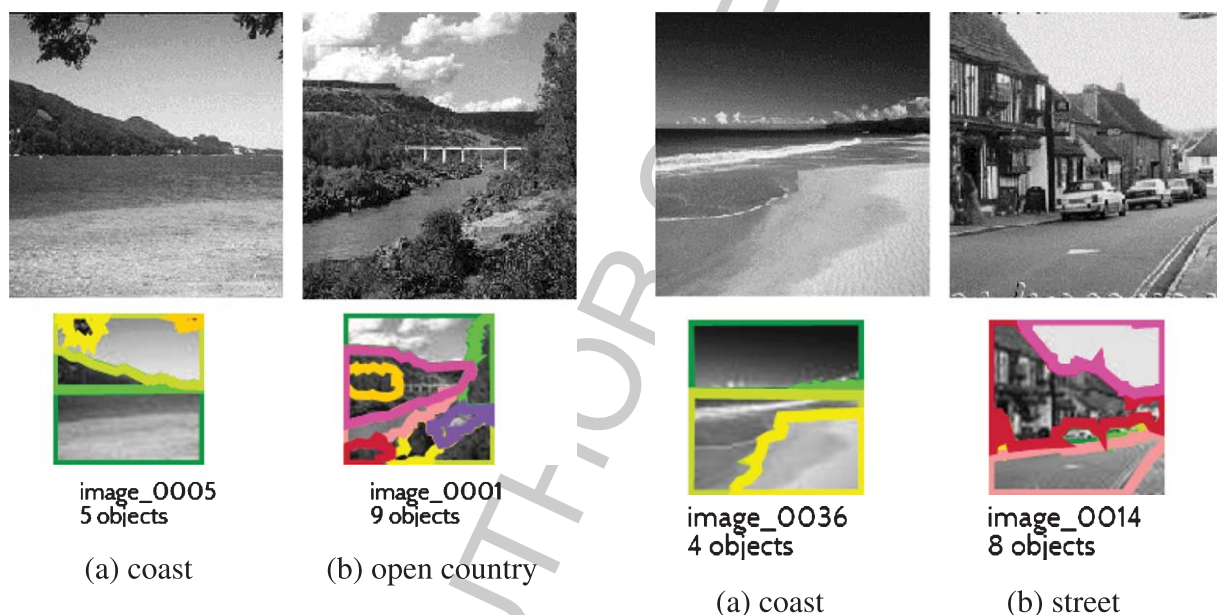


Fig. 7. An example of images from coast and open country scene classes with annotated objects.

Table 7
Membership function for coast and open country scene classes

	Coast	Open country
Sand	0.000	0.056
Water	0.560	0.122
Sky	0.254	0.281
Tree	0.046	0.348
Mountain	0.140	0.193
Vehicle	0.000	0.000
Road	0.000	0.000
Building	0.000	0.000
People	0.000	0.000

scene while the other is *street* scene. Table 8 also shows quantitatively there are no common features (except the universal feature *sky*) that is shared between *coast* and *street* images.

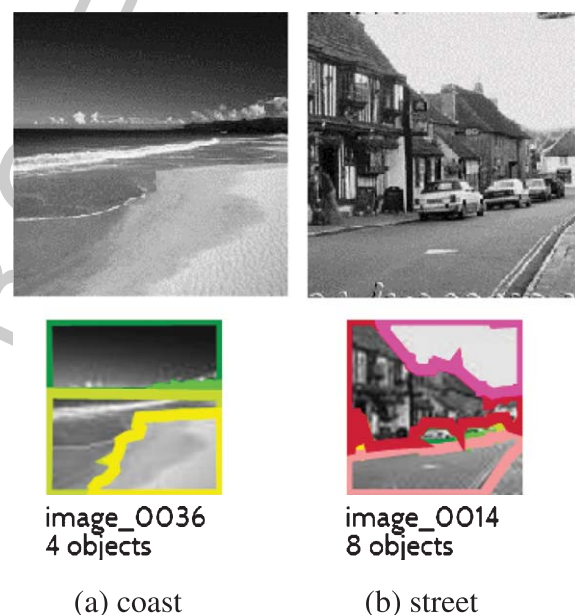


Fig. 8. An example of images from coast and street scene classes with annotated objects.

With the improvements from K7 and K9, this problem was solved. From these improvements, K9 is much more consistent than K7 for scene classification. In Table 4, K9 achieves 100% precision where it was able to classify all the *coast* images as *coast* class, while K7 only achieves 85% accuracy. In Table 5, K9 presents 95% accuracy compared to 20% by K7 in recognizing *open country* images as *open country* class. In Table 6, both K7 and K9 share the same results.

One of the advantages of our proposed approach is that it is able to model the non-mutually exclusive data. Whereby it allows an image to belong to multiple classes as opposed to [5, 12, 15, 18, 23, 24] where the

Table 8
Membership function for coast and street scene classes

	Coast	Street
Sand	0.299	0.000
Water	0.324	0.000
Sky	0.336	0.234
Tree	0.000	0.000
Mountain	0.041	0.000
Vehicle	0.000	0.069
Road	0.000	0.266
Building	0.000	0.419
People	0.000	0.012

classification result is in binary terms. From Table 4 it is observed that when *open country* scene images were tested against *coast* scene, 14 images were accepted to be *coast* by K9. This means an image from *open country* scene class can belong to a *coast* scene as well, as shown in Fig. 7.

4.3. Performance evaluation

In general, there are several standard evaluation metrics available such as precision, recall, accuracy, F-measure, etc. However, the performance evaluation of the multi-label classification problem (our proposed method) is different from the evaluation of uni-label scene classification problem in the sense that in the multi-label classification the output result can be fully correct, partially correct, or fully incorrect [6], making the process a little complicated. For example, say we have three classes $\{c_1, c_2, c_3\}$, and a scene image belongs to c_1, c_2 with a certain degree. Then following results are possible: c_1, c_2 (fully correct); c_1 (partially correct); or c_3 (fully incorrect), results differing from one another in their degree of correctness. In order to evaluate the performance of our proposed scene classification framework, we employed α -evaluation criteria as in [6].

α -evaluation: Let Y_i be the ground truth labels for the test image samples i , and let P_i be the set of prediction labels from the classifier. Then, using α -evaluation, each prediction is given scores using the following formula:

$$score(P_i) = \left(1 - \frac{|\beta M_i + \gamma F_i|}{|Y_i \cup P_i|}\right)^\alpha \quad (14)$$

$$\forall \alpha \geq 0, 0 \leq \beta, \beta = 1 | \gamma = 1$$

where, $M_i = Y_i - P_i$ denotes the missed labels, and $F_i = P_i - Y_i$ denotes the false positive labels. The parameters (α, β, γ) allows the false positives and the misses

Table 9

Example of scores as a function of β and γ when the true label is $\{c_1, c_2, c_3\}$, and $\alpha = 1$. c_1 : coast, c_2 : open country and c_3 : street

	Parameter values	Scores
$\alpha = 1$	$\beta = 0.25, \gamma = 1$	0.9000
	$\beta = 1, \gamma = 1$	0.8500
	$\beta = 1, \gamma = 0.25$	0.9125

Table 10

Example of α -evaluation scores as a function of α when the true label is $\{c_1, c_2, c_3\}$.

	Parameter values	Scores
$\beta = \gamma = 1$	$\alpha = 0$	1
	$\alpha = 0.25$	0.9602
	$\alpha = 0.50$	0.9220
	$\alpha = 0.75$	0.8852
	$\alpha = 1$	0.8500
	$\alpha = 2$	0.7225
	$\alpha = 10$	0.1969
	$\alpha = \infty$	0

Table 11

Comparison of the BK subproduct approach based scene classification with other popular classifiers (in terms of scene understanding)

Classifier	Multi-label	Multi-class
K-nearest neighbour	No	Yes
SVM	No	No
Ours	Yes	Yes

to be penalized differently according to the application. Table 9 shows the results after performing α -evaluation on our proposed method, showing how the score varies with different β and γ values. If we set $\beta = \gamma = 1$, simpler formulation is obtained:

$$score(P_i) = \left(\frac{|Y_i \cap P_i|}{|Y_i \cup P_i|}\right)^\alpha \quad \forall \alpha \geq 0 \quad (15)$$

Table 10 shows some examples of the effect of α on the score. Also, to test the feasibility of our proposed method, we performed comparison on the BK subproduct based scene classification approach with popular classifiers such as K-nearest neighbour and SVM in Table 11. Our proposed method supports both multi-label as well as multi-class classification problem, whereas K-nearest neighbour only supports multi-class, and SVM is neither supporting multi-label nor multi-class. In terms of overall computational complexity, our method takes $O(NM)$ time where N is the total number of scene classes, and M is the total number of features.

5. Conclusion

In this paper, we proposed a framework for natural scene classification that employed inference structures developed from the BK subproduct. We also implemented an improved BK subproduct approach towards scene classification. Experimental results show that a combination of inference structures K7 and K9 work well in forming the inference engine for scene classification i.e. tracing the indirect relationship between the images and the scene classes. The advantages of our proposed approach include: the ability to model the non-mutually exclusive data where it allows an image to belong to multiple scene classes; and the classification results are not binary instead it classifies each scene image as a combination of different classes using the membership function. As future work, we aim at testing our method using a large dataset of both indoor and outdoor scene images for better classification results, and also extending the fuzzy BK subproduct to type-2 fuzzy.

Acknowledgement

This research is supported by the University Malaya Research Grant (UMRG) Grant RP023-2012D, H-00000-56657-E13110 from the University of Malaya.

References

- [1] W. Bandler and L. Kohout, Fuzzy power sets and fuzzy implication operators, *Fuzzy Sets and Systems* **4**(1) (1980), 13–30.
- [2] W. Bandler and L.J. Kohout, Semantics of implication operators and fuzzy relational products, *International Journal of Man-Machine Studies* **12**(1) (1980), 89–116.
- [3] E. Barrenechea, H. Bustince, J. Fernandez, D. Paternain and A. Sanz José, Using the choquet integral in the fuzzy reasoning method of fuzzy rule-based classification systems, *Axioms* **2**(2) (2013), 208–223.
- [4] T. Belicek, J. Kidery, J. Kukal, R. Matej and R. Rusina, Morphological analysis of 3D SPECT images via nilpotent t-norms in diagnosis of Alzheimer's disease, *Journal of Intelligent and Fuzzy Systems* **24**(2) (2013), 313–321.
- [5] A. Bosch, A. Zisserman and X. Munoz, Scene classification via pls, in: *European Conference on Computer Vision (ECCV)*, 2006, pp. 517–530.
- [6] M.R. Boutell, J. Luo, X. Shen and C.M. Brown, Learning multilabel scene classification, *Pattern Recognition* **37**(9) (2004), 1757–1771.
- [7] H. Bustince, P. Burillo and F. Soria, Automorphisms, negations and implication operators, *Fuzzy Sets and Systems* **134**(2) (2003), 209–229.
- [8] T. Chaira, Intuitionistic fuzzy color clustering of human cell images on different color models, *Journal of Intelligent and Fuzzy Systems* **23**(2) (2012), 43–51.
- [9] B. De Baets and E. Kerre, Fuzzy relational compositions, *Fuzzy Sets and Systems* **60**(1) (1993), 109–120.
- [10] D. DeKruger, J. Hodge, J.C. Bezdek, J.M. Keller and P. Gader, Detecting mobile land targets in lidar imagery with fuzzy algorithms, *Journal of Intelligent and Fuzzy Systems* **10**(3) (2001), 197–213.
- [11] C.K. Lim and C.S. Chan, Fuzzy set and multi descriptions property, in: *IEEE International Conference on Fuzzy Systems (FUZZ-IEEE)*, 2012, pp. 1–8.
- [12] F.-F. Li and P. Perona, A bayesian hierarchical model for learning natural scene categories, in: *IEEE Conference on Computer Vision and Pattern Recognition (CVPR)*, 2005, pp. 524–531.
- [13] C.K. Lim and C.S. Chan, A weighted inference engine based on interval-valued fuzzy relational theory, *Expert Systems with Applications* **42**(7) (2015), 3410–3419.
- [14] L.J. Kohout and W. Bandler, How the checklist paradigm elucidates the semantics of fuzzy inference, in: *IEEE International Conference on Fuzzy Systems (FUZZ-IEEE)*, 1992, pp. 571–578.
- [15] S. Kumar and M. Hebert, Discriminative random fields: A discriminative framework for contextual interaction in classification, in: *IEEE International Conference on Computer Vision (ICCV)*, 2003, pp. 1150–1157.
- [16] C.K. Lim and C.S. Chan, Logical connectives and operativeness of bk sub-triangle product in fuzzy inferecing, *International Journal of Fuzzy Systems* **13**(4) (2011), 237–245.
- [17] C.H. Lim, A. Risnumawan and C.S. Chan, Scene image is non-mutually exclusive - A fuzzy qualitative scene understanding, *IEEE Transactions on Fuzzy Systems* **22**(6) (2014), 1541–1556.
- [18] A. Oliva and A. Torralba, Modeling the shape of the scene: A holistic representation of the spatial envelope, *International Journal of Computer Vision* **42**(3) (2001), 145–175.
- [19] H. Peng, J. Wang, M.J. Perez-Jimenez and P. Shi, A novel image thresholding method based on membrane computing and fuzzy entropy, *Journal of Intelligent and Fuzzy Systems* **24**(2) (2013), 229–237.
- [20] C.H. Lim, E. Vats and C.S. Chan, Fuzzy human motion analysis: A review, *Pattern Recognition* **48**(5) (2015), 1773–1796.
- [21] B.C. Russell, A. Torralba, K.P. Murphy and W.T. Freeman, Labelme: A database and web-based tool for image annotation, *International Journal of Computer Vision* **77**(1-3) (2008), 157–173.
- [22] E. Vats, C.K. Lim and C.S. Chan, A BK subproduct approach for scene classification, in: *IEEE Image Electronics and Visual Computing Workshop*, 2012.
- [23] J. Vogel and B. Schiele, Natural scene retrieval based on a semantic modeling step, in: *Third International Conference on Image and Video Retrieval (CIVR)*, 2004, pp. 207–215.
- [24] J. Vogel and B. Schiele, Semantic modeling of natural scenes for content-based image retrieval, *International Journal of Computer Vision* **72**(2) (2007), 133–157.
- [25] K. Yew and L. Kohout, Interval-valued fuzzy relational inference structures, in: *IEEE International Conference on Intelligent Information Management Systems*, 1996, pp. 173–175.
- [26] K. Yew and L. Kohout, Interval-based reasoning in medical diagnosis, in: *IATED International Conference on Intelligent Information Systems*, 1997, pp. 32–36.
- [27] M. Zaki and M. Abulwafa, The use of invariant features for object recognition from a single image, *Journal of Intelligent and Fuzzy Systems* **12**(2) (2002), 79–95.